AUTOMATION OF AN INDUSTRIAL FORK LIFT TRUCK, GUIDED BY ARTIFICIAL VISION, ULTRASONIC AND INFRARED SENSORS IN OPEN ENVIRONMENTS

Manuel Mazo, Francisco J. Rodríguez, Miguel A. Sotelo, Jesús Ureña, Juan C. García, José L. Lázaro, Felipe Espinosa.
Department of Electronic. University of Alcala.
Escuela Politécnica. Campus Universitario s/n 28871 Alcalá de Henares (MADRID). SPAIN.
Telephone +34-1-8854810. Fax +34-1-8854804.
E-mail: {mazo, urena, fjrs, sotelo}@depeca.alcala.es

Abstract

This paper describes the perception and guidance system of a commercial industrial fork-lift truck for applications in industrial environments. A distributed control system was used, where communication between the various nodes making it up is effected by a specific local bus for real time control. The perception system includes, amongst others, ultrasonic and infrared vision sensors that obtain tracking information for the paths the fork-lift has to follow (i.e. roads) and information on the nearby environment. This allows obstacle-free paths to be picked out for the fork-lift to follow.

1 Introduction

One of the most important of the many applications of autonomous mobile robots is transporting products within industrial environments. From the guidance point of view this type of robot normally needs a high and reliable perception capacity allowing it to move safely through different types of routes. Other aspects, albeit to a lesser degree, are obviously also important, such as autonomy, manoeuvrability, ease of loading and unloading, maximum load, etc.

It goes without saying that, just as with living beings, the more complicated the sensory system is, the easier it is to endow the mobile robots with a greater autonomy. This allows them to move along different types of paths or at least means that any change of path does not involve a costly investment, besides allowing them to move with greater safety and carry out more complex tasks. The main objective of the sensory system is to endow the mobile robot with the capacity of reliable and accurate on-line perception of the environment surrounding it. The work herein presented comes within the field of perception and guidance systems for mobile robots. Specifically, results are presented of research work carried out in the Electronics Department of the University of Alcalá, the main objective of which was to equip a commercial industrial vehicle (industrial fork lift truck) with a perception and control system that would allow it to move along road-type paths, detecting and skirting any obstacles as they cropped up. Figure 1 shows the external aspect of the industrial fork-lift truck used. It has been equipped with a control system including different nodes. Each node has enough processing capacity to endow it with a certain autonomy. These different nodes include those of low-level control (control of drive and steering motors), capture and processing of the information provided by the various sensors, high-level control, path generation, etc.

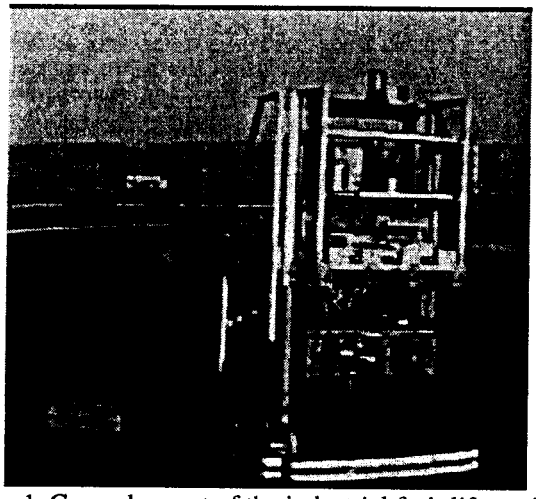

Figure 1. General aspect of the industrial fork-lift truck used in the experiments.

2 Architecture

The control architecture used on the industrial fork-lift truck is shown in figure 2, highlighting the nodes:

a) Control system for drive and steering motors: This electronic module controls linear and angular movements of the robot, thanks to the feedback provided by the encoders coupled to the different axles.

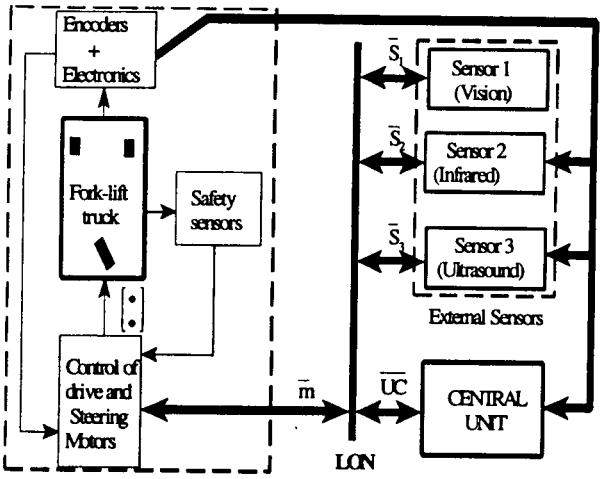

Figure 2. Control architecture.

b) Safety sensors: these come into operation in extreme conditions when there is a risk of collision.

c) Dead-reckoning system (encoders plus electronics). A card (Ureña 96) to process the information coming from the different encoders gives periodic (every 10 ms) information on the position and speed of each of the fork-lift's axles. This information then allows the system to keep progressive track of the position of the "centre" of the fork-lift.

d) Intermediate control system (central unit): This module processes the high-level "commads" of the different sensors and then adapts them, according to the pre-eminence of each one, to low-level commands (steering position and angular speed of the drive wheel), which can be suitably interpreted by the motor control card. Also taken into account at this point are the physical model of the robot and the type of control it is wished to exert over it, etc.,

e) Ultrasonic sensor system: These sensors serve to detect the presence of obstacles or objects in the environment around the robot. A first interpretation of the data obtained from these sensors allows the robot to avoid obstacles. A more detailed analysis then enables the objects to be identified plus the position of the vehicle with regard to those obstacles.

f) Infrared sensor system: This system enables certain sectors of the vehicle's environment to be modelled three-dimensionally (3D models), as well as giving its position with respect to external beacons suitably laid out.

g) Artificial vision system: This gives visual information on the fork lift's environment, allowing it to be guided along road and similar communication routes by picking out their verges.

h) Communication bus: In a system of this type the communication between the aforementioned modules is fundamental. As each block has enough intelligence to carry out a large part of the processing of the exterior information received, the number of messages mutually interchanged between them is not great. In the chosen bus, therefore, stress has been laid on the real-time, reliable communication of a moderate amount of data. A bus that fits this performance profile, facilitating at the same time the configuration and flexibility of the system, is the ECHELON (ECHELON 93). In this bus each node has a link circuit called "Neuronchip" that, by means of a high-level language (Neuron C), enables the system to be configured (identifying which variables are shared with other nodes) and communications to be established.

3. Description and modelling of the fork-lift truck

The industrial fork-lift truck that serves as platform for effecting the work herein presented is a standard industrial fork-lift truck (Asti,95) as shown in figure 1. It has a depth - D - of 1.100 m., a length - L - of 1.700 m., and a height -H- of 2.000 m. It is mounted on three wheels, two fixed non-drive wheels (placed in parallel on the sides at the rear) and one drive-steering wheel in the middle at the front (1.275 m from the imaginary axle linking the two back wheels). Its structure is therefore basically that of a tricycle. All wheels have a radius - R - of 0.1m. The fork-lift incorporates different types of sensors (safety sensors, vision sensors, ultrasonic and infrared sensors, etc) and all the electronics designed ad hoc by our Department for the control of the motors and the processing of the sensory information. Although the complete modelling of any mobile robot has to be characterised by its kinematic and dynamic behaviour (Sarkar et al, 94) (DeSantis, 95), given that the vehicle involved here is an industrial vehicle running at low speeds, the control and guidance thereof can in this case be based on a kinematic model alone, without taking into account acceleration, inertia and reaction forces of the robot-ground contact or the wheels-platform contact. (Steer and Larcombe, 91), (Reister, 92).

The model used therefore relates the overall values: longitudinal speed V and angular speed of the robot (from which the XY position and orientation are derived), to the local values: steering angle and driving speed (Muir and Neumann, 87). The vehicle is moved at a constant linear and angular speed around the instant curvature radius ICR (figure 3). This is the point where the lines perpendicular to the wheel plane that passes through the midpoint of the wheels cross. Thus the components of linear speed V_r in the mid point between the back wheels, V_f in the drive wheel and V in the mass centre are vectors perpendicular to the imaginary axis uniting said points with the ICR. In accordance with the geometric parameters shown in figure 3 the following relations can be established with said linear speeds and the angular speed of the robot:

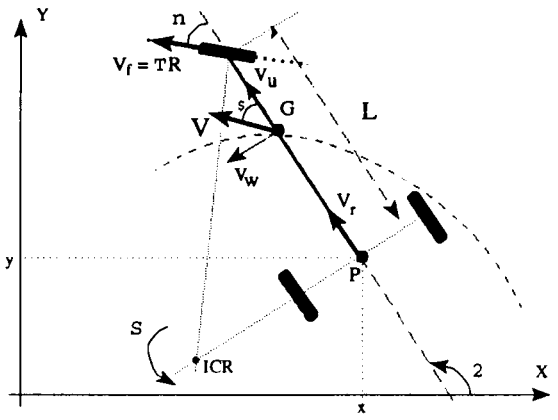

Figure 3. Relevant parameters and variables of the kinematic modelling of the industrial fork-lift truck.

$$|V_f| = \omega R \qquad \angle V_f = \varphi$$

$$V_f = V_r + \Omega \wedge L$$

$$V_f = V + \Omega \wedge L_f$$

where L_f is the distance between the drive wheel and the mass centre. If the centre line between the back wheels P is taken as reference point, the following obtains:

$$\frac{dx}{dt} = \omega R \cos\varphi \cos\theta$$

$$\frac{dy}{dt} = \omega R \cos\varphi \operatorname{sen}\theta$$

$$\frac{d\theta}{dt} = \frac{\omega R}{L} \operatorname{sen}\varphi$$

4 Artificial Vision System

The main guidance system is based on artificial vision techniques for calculating the right-hand verge of the paths marked out as roads. This verge is the robot's fundamental reference for tracking the road or path it is moving along. In well-marked paths detection of the verges poses no great problem, except in adverse weather conditions. There are, however, many roads with no painted lines, where there is no option but to resort to differentiating characteristics. The main drawback of textural techniques is the long computing time and the difficulty of adapting to sudden changes in lighting conditions or the appearance of strong shadows. An alternative is to opt for a search for another type of characteristics with a lower computing time and with less sensitivity to lighting conditions. This is the case when working with video signals taken by a colour camera.

4.1 Study of the Image

To study the image provided by the camera, a zone of interest is set up called the active zone, upon which calculation of the road verge is centred. The image is therefore pre-processed beforehand.

4.2 Pre-processing

The first operation carried out on the road image is a pre-processing based on colour bands to smooth out the effect of shadows and holes in the road. Figure 4 shows an example in which the shadows are attenuated by the pre-processing of the image.

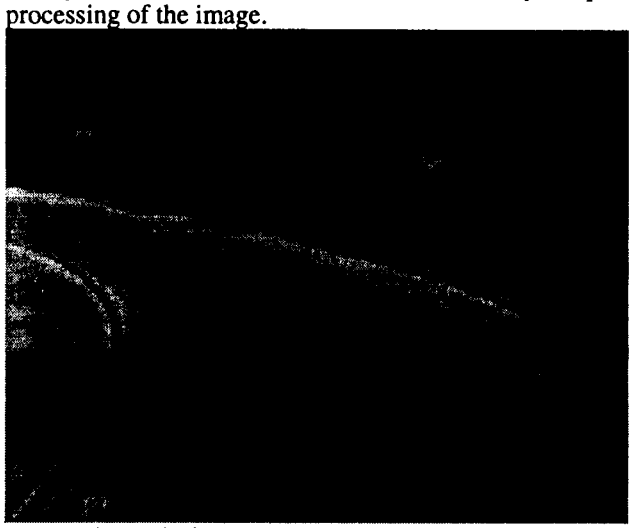

Figure 4. Example of Pre-processed Image.

To do so, the shine is standardised in the B band (blue), but to avoid the elimination of discriminating factors of crucial importance a term is added representing the absolute contents of the blue colour band (Pomerlau, 93). The final pre-processed image eliminates or at least attenuates the effect of shadows in the road and is obtained with the following equation:

$$p = \frac{B}{255} + \frac{B}{R+G+B}$$

4.3 Active zone

The image provided by the camera is scaled by real time hardware procedures to a size of 320 x 240 pixels. After various practical tests a zone is established within the image called the *active zone*, considered as the zone of interest (Rodriguez F.J. et al, 94). This zone has a size of 320 x 120 pixels. The active zone of the image is subdivided into windows of 10 x 10 points for studying the properties of each one. The aim is to segment the active zone into windows belonging to the road (the path to follow) and non-road windows. This gives a low resolution black-and-white image wherein the calculation of the verges is simpler.

4.4 Selection of characteristics

Each colour image point may be defined by five characteristics, the three colour bands (R,G,B) and the co-ordinates of the point within the image (i,j). Working from this vector, it is necessary to establish whether or not the information provided by these characteristics is redundant. A selection of characteristics is therefore

made by carrying out an exhaustive search to minimise the classification error, measured in terms of a classifier built up from the total of the samples less one used to conduct the tests. Tests were therefore carried out on a varied set of images including most of the situations that usually arise in road tracking; different types of asphalt, lighting changes, shadows, etc. The main conclusions drawn from the selection tests are given below:

- In most cases the R and B bands suffice to separate correctly road from non-road, including images with shadows. It is thereby confirmed that the combination of these bands can serve for building up an image wherein shadows are greatly attenuated..
- The pixel co-ordinates diminish the classification error for points located in the centre of the image, normally always belonging to the road. But they increase it for verge points, since the condition of the latter is that which is most affected by changes in the road direction. It is therefore best to avoid using pixel co-ordinates as characteristics.

Final results advocate the use of the R and B bands as discriminating characteristics for classifying the windows of the active zone of the image.

4.5 Discriminating Analysis

After obtaining the characteristics vector of each window, calculated as the mean of the R and B values of the pixel making it up, the windows should then be correctly classified. A classifier is therefore constructed based on the discriminating analysis theory. The classifier must allow the continuous adaptation of the parameters as the road tracking is carried out. A statistical classifier was used, specifically the Bayesian classifier, whose principal virtue lies in its capacity for improving recognition among overlapping classes. The density function of the samples is assumed to be gaussian.

$$f(\bar{x}) = \frac{1}{2\pi |C_i|} \exp\{-\frac{1}{2}(\bar{x}-\bar{m}_i)^T C_i^{-1}(\bar{x}-\bar{m}_i)\, p(\alpha_i)\}$$

where α_i represents the class i, C_i is the covariance matrix of all the samples of a given class and m_i is the average vector thereof. Taking neparians of the probability density function, we obtain the following equation:

$$f_d(\bar{x}) = k_i + \omega_i^T \bar{x} + f(\bar{x}^T \bar{x})$$

If the classes share equiprobability and the covariance matrices of the samples forming them are equal, the third sum may be dispensed with, thereby obtaining a linear discriminating function.

Adaptation of the discrimnating functions

In the first iteration of the algorithm the discriminating functions are calculated for the two classes (road and non-road) with the information taken from an alternative algorithm or by direct supervised indication. After carrying out the classification and obtaining the road verges the discriminating functions are updated in terms of the calculated road position (Rodriguez F.J et al, 94). The aim is to obtain the new characteristics of the image studied so that they serve as a classification pattern in the next iteration of the algorithm. Therefore, if the sampling period is sufficiently small, the path marked by a road can be followed, even if its characteristics vary, as they are updated in each iteration of the algorithm. Figure 5 shows an example of an image segmented by the discriminating classifier developed.

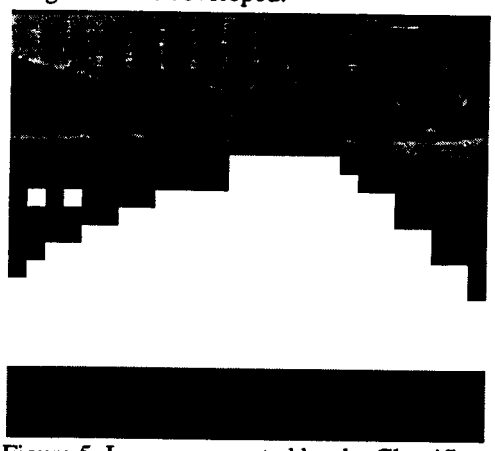

Figure 5. Image segmented by the Classifier

4.6 Obtaining the verge.

The low-resolution segmented image is then used to obtain all the verge points of the image by applying a simple high-pass filter. The problem now lies in identifying which of them really correspond to the road verges. The road verge is modelled as a second-order equation in which the three coefficients thereof , *a, b,* and *c,* have to be identified in each case. First it is necessary to search for the potential verge points within the image. The search starts with an initial model (a_0, b_0, c_0) setting up an exploration margin around it. All points coming within said zone are deemed to be road verge points. With the points found the new road state has to be estimated, i.e., the new values of the coefficients. The estimation method used was based on Weighted Recursive Least Squares with Decreasing Exponential. In the recursive formulation of this method the current solution receives the name of state (a, b, c). When a set of verge points of an image are obtained, the state is recalculated using only this data explicitly. Past data are completely represented by the previous state and the estimated covariance in the previous state. The updating involves three successive calculations.

a) Prediction updating:

$$\hat{y}(t) = \phi^T(t)\theta(t-1)$$

b) Updating of the estimated covariance:

$$P(t) = \frac{1}{\lambda}\{P(t-1) - (P(t-1)\phi(t)\cdot(\lambda I + \phi^T(t)P(t-1)\phi(t))^{-1}$$

$$\phi^T(t)P^T(t-1))\}$$

where:

$$y(t)=\begin{pmatrix} x_{t,1} \\ x_{t,2} \\ \cdots\cdots \\ x_{t,N} \end{pmatrix} \qquad \phi^T(t)=\begin{pmatrix} 1 & y_{t,1} & y^2_{t,1} \\ 1 & y_{t,2} & y^2_{t,2} \\ \cdots & \cdots\cdots & \cdots\cdots\cdots \\ 1 & y_{t,N} & y^2_{t,N} \end{pmatrix} \qquad \theta(t-1)=\begin{pmatrix} c \\ b \\ a \end{pmatrix}$$

c) Updating of estimated state:

$$\theta(t)=\theta(t-1)+P(t)\phi(t)(y(t)-\hat{y}(t))$$

where θ(t-1) represents the estimated state at the moment t-1 and P(t-1) represents an estimate of its covariance. Figure 6 shows an example of a road verge calculated by this method.

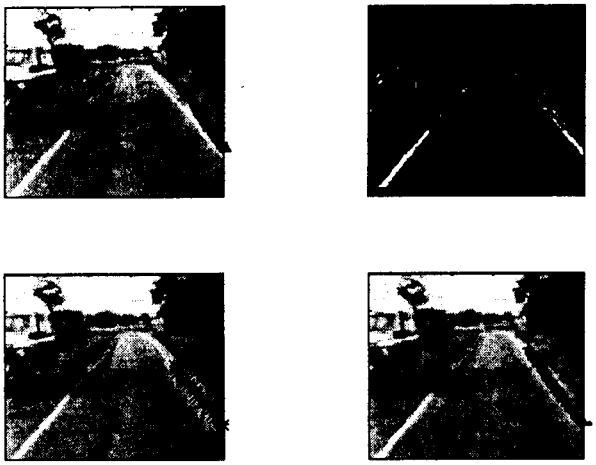

Figure 6. Road verge found by the least squares method.

4.7 Tests and Results

Two main types of tests were conducted to verify the algorithm's validity. Firstly, video recorded images were used to simulate the laboratory process. Results were satisfactory, table 1 showing the measured error and the number of points found during the tracking of a section of road with various right-hand and left-hand bends and straight sections

Table 1. Video tape results.

Image N°	Image type	Error(%)	N° of points
1	Straight	11.21	11
2	Right	13.82	12
3	Right	12.54	12
4	Right	9.97	12
5	Straight	21.55	11
6	Left	23.14	12
7	Left	14.81	12
8	Left	12.54	11
9	Straight	17.34	10
10	Straight	11.03	12

The Table shows that the number of verge points found in each case is quite high, so the error is not excessive in most of the images. Test were also carried out in outside spaces. The fork-lift truck was tried out on the campus of the Universidad de Alcalá. The maximum guidance speed reached by the fork-lift is 2 m/s, although in most tests an average speed of 1 m/s was obtained. Figure 7 shows the result of the path tracked by the fork-lift in one of the tests.

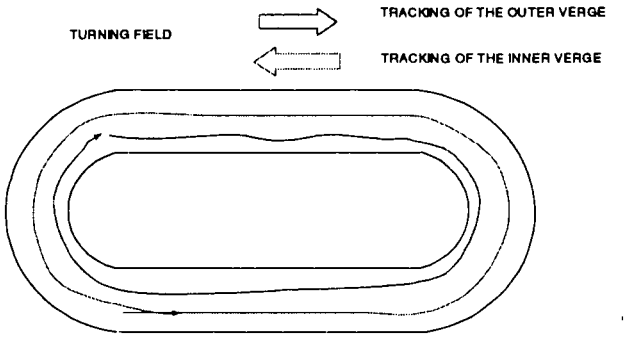

Figure 7. Path tracked by the fork-lift in outside tests.

5 Ultrasonic Module

The complete sonar node is shown in the block diagram of figure 8. It allows the handling of sensors comprising four transducers each (Ureña et al, 1998) (20 transducers were fitted to set up a total of 5 sensors). The modular electronic architecture provides great flexibility, and has been designed to allow three different levels of information processing:

Low level: A two-phase modulation is carried out at transducer level (with a 50 KHz carrier) of a suitably chosen digital sequence (13 bit Barker code). The signal received is digitalised (at 500 Khz) and processed to obtain, accurately and practically without delay, the times of flight of the ultrasounds corresponding to the most significant echoes. The digital processing of the signal is carried out on an FPGA, thereby obtaining the validation of an echo in 584 ms after the start of its reception.

Mid level: Each four transducers function as a single sensor, so they all receive an echo signal even when only one of them was the actual emitter of it. A micro-controller synchronises the four transducers, calculates the times of flight and groups the echoes in terms of the correspondence between them (observing that the difference detected between them is less than d/csina where c is the speed of the ultrasounds in the air, d the separation between transducers and a the half angle of the emission/reception standard). For this purpose, only the first four echoes received by each sensor, at most, will be considered.

High level: The configuration of each of the sensors (identifying which transducers measures, in which order and with what cadence), as well as the overall data collection is effected by another electronic board with a main micro-controller housed in the expansion bus of a PC. It shares a common storage zone with the latter(dual-port), directly addressed by both. Each time a reading is begun with the ultrasounds, the micro- controller takes the value of the robot's position from the odometer and

then stores it together with the data obtained. The PC reads all this information to process it, without the need for any datum-by-datum synchronisation with the microcontroller (the last 8 complete sweeps of the sonar system are stored). From the PC, through this same storage, the functioning of the whole sonar node may be configured. Another specific PCLTA board, also housed in the PC, provides access to the LONWORKS bus (García J.C. et al, 1997).

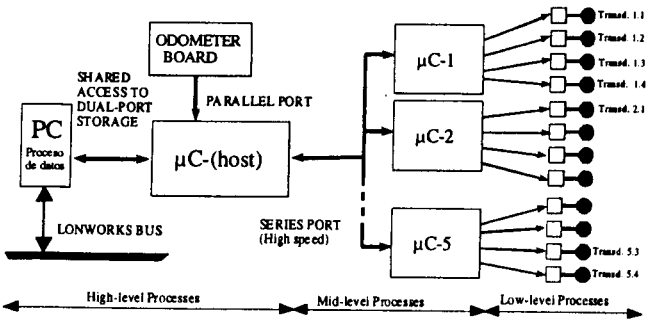

Figure 8. Block diagram of sonar node.

5.1 roccessing of the sonar information

Figure 9 shows the distribution of the five sensors and the area swept by them.

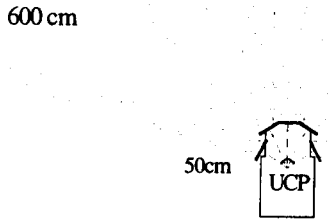

Figure 9. System and zone covered by the sensors.

Analysis of the inter-echo correspondence (verification of whether the transducers have detected the same reflector or another very nearby one) gives a general rule such as the one shown in Table 2 (Ureña et al, 1998). The sensor was simplified, given that each two transducers at the ends are close enough to be assumed to take in the same zone (see Figure 10). When the location of points A and B is known, plus the orientation of the transducers, the values resulting from a given reading determine which zones in front of the sensor may be considered as "vacant" of obstacles and which "occupied", for the purposes of mapping and guidance aid. In the algorithm proposed herein, based on the HAM (Song & Chen, 1996) not only the distance measured is taken into account but also whether the distance measured is confirmed by the two end transducers (double confirmation)

- in the event of discrepancy the lower distance is chosen
- whether the listening angle has been obtained (maximum certainty is assigned thereto) and whether the reflector type has been determined (if it is a wall consideration is given to its angle of inclination to determine the "full" zone.

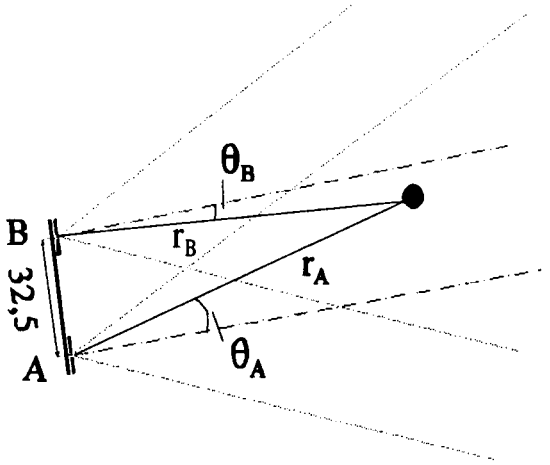

Figure 10. Simplification of each sensor

Table 2.- Data obtained from one reading.

Correspondence between: R1-R2	R3-R4	R1-R4	Obtaining:
No	No	Indifferent	r_A and r_B
No	Yes	Indifferent	r_A, r_B and θ_B
Yes	No	Indifferent	r_A, θ_A and r_B
Yes	Yes	No	r_A, θ_A, r_B and θ_B
Yes	Yes	Yes	r_A, θ_A,, r_B,, θ_B and type

For both zones the following grid updating function (f) is used to build up the map:

$$f = \left[1 - \frac{r - d_{min}}{2 \cdot (d_{max} - d_{min})}\right] \cdot e^{-\left[\frac{(\theta - \theta_c)^2}{2 \cdot \sigma^2}\right]}$$

where (r θ) is the point of the "vacant" or "full" zone considered (with respect to A or B as the case may be) d_{min} and d_{max} are the minimum and maximum distances processed, θ_c is the listening angle detected and σ is the value representing how far the function is from its maximum (fixed at 5^0 for the full zone if it is not a wall and 30^0 if it is a wall, being 10^0 for the vacant zone in both cases). This function is applied to the central point of each cell of the environment

$$CV(k) = m \cdot f + (1 - m) \cdot CV(k - 1)$$

where m is a factor between 0 and 1 that considers the influence of the past history in the map updating. In accordance with the empirical considerations of the HAM

method 0.4 was chosen for the "full" zone and 0.2 for the "vacant" zone. Evaluation of the aforementioned *f* function was done off line for all existing cells in an octant of the co-ordinate system centred on the transducer position. Remaining octants can then be dealt with by an easy extrapolation based on symmetry considerations. A first template was thereby generated for each reading that assumed an orientation - according to the main axis - and distance coinciding with the cell in question. Furthermore, for each cell consideration was given to additional templates taking into account the angles measured (discriminated to values -12, -9, -6, -3, 0, +3, +6, +9, +12).

6 Infrared Module

One technique for modelling an unknown environment in which a mobile robot is to be guided, involves obtaining 3D co-ordinates by emitting structured light and capturing it in a CCD camera. Beforehand, the whole system (camera and emitted light analyser) has to be jointly calibrated with reference to the same co-ordinates origin [Jarvis, 83]. The distance maps obtained may be used to deduce vacant, occupied and safety zones, generating paths that are updated according to the characteristics of the captured field of view to reach a final position. From the many path options, that should be chosen which gives some guarantee of safety while also observing the path to be followed.

6.1 CCD-laser coupling and obtaining 3-D co-ordinates

The general method for obtaining the 3D co-ordinates involves solving the system of equations obtained from the camera model (for each point registered that belongs to those emitted by the laser in plane form) , and the equation of this plane . This gives three equations that in turn give the x,y,z co-ordinates:

camera mod *el* $a_1x+b_1y+c_1z+d_1=0$

$a_2x+b_2y+c_2z+d_2=0$

plane: $Ax+By+Cz+1=0$

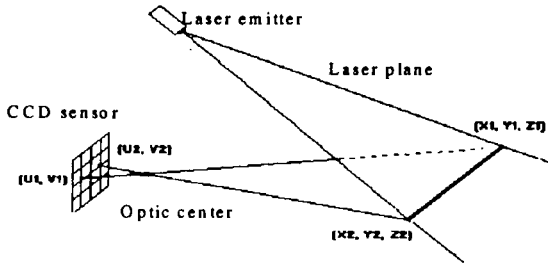

Figure 11. Obtaining the plane equation.

The aim of the emitter-camera coupling is the modelling and calibration of the system [Chen and Ni, 93], with respect to the same reference and with the minimum error. In principle it is necessary to have an optical system coupled to the sensor, which must be perfectly linear. Before the calibration a study is made of the optimum position of emitter and detector, so that the most is made of the qualities and resolution of the latter

Before obtaining the plane equation it is necessary to eliminate from the image everything that does not belong to the light emitted by the laser and reduce the thickness of same to a pixel. Firstly an optical filter is used to eliminate all possible light except the wave length emitted as structured light. An active search is made for very bright points belonging to the laser and a "kernelling" of the image is carried out, stressing points belonging to horizontal or near-horizontal lines and the threshold is then set. Then all those points not belonging to narrow beams are eliminated.

6.2 Definition of the virtual space

With the information on the environment provided by the perception system (co-ordinate matrix) an analysis is made of the make up of the environment with a sufficient depth (safety distance) to be able to react in the face of any obstacles. Due to the great number of points analysed [Foux *et al*, 93], they are previously filtered to unify values of adjacent points, thereby deducing vacant and obstructed zones in a first sectorisation.

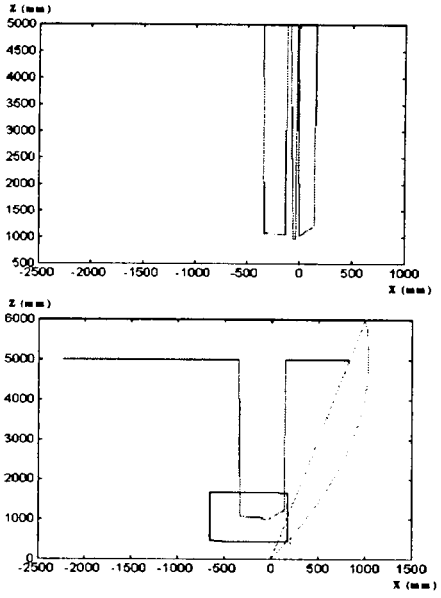

Figure 12. Detection of obstacles and calculation of virtual obstacle.

After these steps the detected outline of the obstacles is generated, modifying it if it presents concavities, since this would guide the robot into a cul de sac or cause it to make unnecessary movements Now the problem is tackled of determining where the robot may be set up in terms of its orientation and dimensions, and how to move it from one position to another without producing collisions. The solution adopted is to widen the intermediate

objects in each iteration, in accordance with the size of the robot and the direction it is moving in, considering it as a one point .

7 Conclusions

A distributed control system and a sensory system based fundamentally on three sensor types was developed and put into practice on a standard industrial fork-lift truck; this system guaranteed the autonomous guidance in industrial environments. Tests proved that visual information in colour captured by a camera makes it possible to segment the path to follow, the latter being defined as a road. The algorithms used guarantee the segmentation even in poor lighting conditions and/or poor definition of the path to follow. Tests carried out and the results thereby obtained bear this out.

The proposed ultrasonic sensor model guarantees good results in the detection and classification of the obstacles that may crop up. This guarantees the obtaining of obstacle-free spaces through which the robot may pass. A further contribution to this is made by the infrared system which guarantees high accuracy and reliability in obtaining the 3D information of the environment closest to the fork-lift.

It was demonstrated that with the proposed system (sensors + control) an industrial vehicle may track paths defined as roads within industrial environments. The system may also be transferred with no great modifications to other types of commercial industrial vehicles different from that described herein.

8 Acknowledges

The authors wish to express their gratitude to CICYT (Interministerial Science and Technology Commission) for the aid received through the project TAP94-0656-C03-01 thanks to which the research work described herein was carried out.

References

[Sarkar et al, 94] Sarkar,N., Yun, X., Kumar,V. *Control of Mechanical Systems with Rolling Constrains: Application to Dynamic Control of Mobile Robots.* The International Journal of Robotics Research. Vol. 13. N° 1. February 1994.

[DeSantis, 95] DeSantis, R.M. *Path-tracking for Car-Like Robots with Single and Double Steering.* IEEE Transactions on Vehicular Technology. Vol.44, N°2, May 1995.

[Steer and Larcombe, 91] Steer, B., and Larcombe, M. *A goal Seeking and Obstacle Avoiding Algorithm for Autonomous Mobile Robots.* Proceedings of the IEEE International Conference on Robotics and Automation. Sacramento, California. April, 1991.

[Reister, 92] Reister, D.B. *A new wheel control system for the omnidirectional HERMIES III robot.* Robotica.Vol. 10 pag. 351-360.

[Muir and Neuman, 87] Muir, P. F. and Neuman, C. P. *Kinematic Modeling of Wheeled Mobile Robots* Journal of Robotic Systems. Vol. 4, N°2, pag 281-340. 1987j.

[Pomerleau, 93] Pomerleau D. *Neural Network Perception for Mobile Robot Guidance*, Kluwer. Boston. 1993.

[Rodríguez et al, 94] Rodríguez F. J, Mazo M., Sotelo M.A. and Santiso E., *Road following by artificial vision using neural network.* International Symposium on Artificial Intelligence in Real Time Control. pp. 263-268. October 1994.

[Song and Chen, 96] Song K.T. y Chen Ch. Ch. *Application of Heuristic Asymmetric Mapping for Mobile Robot Navigation Using Ultrasonic Sensors.* Journal of Intelligent and Robotics Systems. Vol. 17, pp. 243-264, 1996.

[Ureña et al, 98] Ureña J., Mazo M., García J.J. y Bueno E. *Ultrasonic Sensor Module for an Autonomous Industrial Vehicle.* 3rd IFAC Symp. on Intelligent Autonomous Vehicles (IAV'98) . Madrid, March 1998. Accepted.

[García et al, 97] García J.C., Marrón M., García J.A., Ureña J. Lázaro J.L., Rodríguez F.J., Mazo M., Escudero M.S. *Application of LonWorks Technology to Low Level Control of an Autonomous Wheelchair.* LonUsers International Spring'97 Conference & Exhibition. Santa Clara (USA) May 1997.

[Jarvis, 83] Jarvis, R.A. *A perspective on range squematizacion finding techniques for computer vision.* IEEE Transactions on Pattern Analysis and Machine Intel, Vol. PAMI-5, NO. 2, Mar 1983.

[Chen and Ni, 93] Chen, Y. D. and Ni, J. *Dynamic calibration and compensation of a 3-D laser radar scanning system.* IEEE Transactions on Robotics and Automation, Vol. 9, NO. 3, Junio 1993.

[Foux et al, 93] Foux. G, Heymann. M and Bruckstein. A. *Two Dimensional Robot Navigation Among Unknown Stationary Polygonal Obstacles.* IEEE Transactions on Robots and Automation. VOL 9. NO 1. February 1993.